http://www.jstage.jst.go.jp/browse/biophysics

BIOPHYSICS

Vol. 7, pp. 77–88 (2011)
doi: 10.2142/biophysics.7.77

Chemophoresis as a driving force for intracellular organization: Theory and application to plasmid partitioning

Takeshi Sugawara[1] and Kunihiko Kaneko[2,3]

[1]*Cell Architecture Laboratory, Center for Frontier Research, National Institute of Genetics, 1111, Yata, Mishima, Shizuoka 411-8540, Japan*
[2]*Department of Basic Science, Graduate School of Arts and Sciences, The University of Tokyo, 3-8-1, Komaba, Meguro, Tokyo 153-8902, Japan*
[3]*Complex Systems Biology Project, ERATO, JST, Komaba, Meguro, Tokyo 153-8902, Japan*

Received July 4, 2011; accepted September 8, 2011

Biological units such as macromolecules, organelles, and cells are directed to a proper location by gradients of chemicals. We consider a macroscopic element with surface binding sites where chemical adsorption reactions can occur and show that a thermodynamic force generated by chemical gradients acts on the element. By assuming local equilibrium and adopting the grand potential used in thermodynamics, we derive a formula for the "chemophoresis" force, which depends on chemical potential gradients and the Langmuir isotherm. The conditions under which the formula is applicable are shown to occur in intracellular reactions. Further, the role of the chemophoresis in the partitioning of bacterial chromosomal loci/plasmids during cell division is discussed. By performing numerical simulations, we demonstrate that the chemophoresis force can contribute to the regular positioning of plasmids observed in experiments.

Key words: thermodynamic force, chemical gradient, chemical adsorption, plasmid partitioning

1. Introduction

Biological entities such as cells, organelles, and macromolecules often move to appropriate locations under an external chemical gradient. In cell chemotaxis, the process by which an organism senses the presence of an external chemical and responds to it has been elucidated in depth. However, the coordinated motion of entities is not limited to those at the organism level. In recent studies, it has been shown that such directional motion under chemical gradients/localizations plays an important role in organization at an intracellular level[1], e.g., microtubule guidance under a RanGTP gradient[2–4] or Stathmin gradient[5], actin nucleation under an IcsA gradient on the outer membrane of a pathogen *Shigella flexneri* (actin comet)[6,7], bacterial chromosomal locus/plasmid DNA partitioning by a Par system[8–24]. However, the general mechanism underlying the coordinated motion of organelles or macromolecules under an intracellular gradient/localization is yet to be understood.

The formation of organelle/macromolecule patterns by chemical concentrations under non-equilibrium conditions, first observed during macroscopic morphogenesis[25], has recently been observed at the intracellular level as well, and its relevance to intracellular organization processes has been demonstrated in the case of bacterial plasmid DNA partitioning by a Par system[11–24], determination of the plane of cell division in bacteria using the Min system[26–36], etc. These studies have discussed how positional information given by the chemical concentration gradient/localization is generated and maintained. However, there are few studies on the role of chemical gradients/localization in the coordinated motion, transport, and positioning of organelles or macromolecules under non-equilibrium conditions.

Corresponding author: Takeshi Sugawara, Cell Architecture Laboratory, Center for Frontier Research, National Institute of Genetics, 1111, Yata, Mishima, Shizuoka 411-8540, Japan.
e-mail: tsugawar@lab.nig.ac.jp

In the present paper, we present a physical mechanism that can explain the coordinated motion and positioning. According to the mechanism, in the presence of a chemical gradient resulting from a reaction, a macroscopic element consisting of a number of reaction sites is generally subjected to a force. By considering this element to be a scaffold that adsorbs chemicals, we derive a formula for the force generated by a chemical potential gradient. In the derivation, we introduce the grand potential used in thermodynamics for an open system. The direction of motion of the element is such that the chemical potential increases. A formula is obtained by assuming that the reaction process reaches equilibrium faster than the motion of the element and by extending the minimization of free energy to include the contact with a particle bath with a given chemical gradient. We propose that the force leads to a general mechanochemical coupling; we call this force *chemophoresis force*. We show that the work done by the chemophoresis force can be much greater than the thermal energy fluctuations. By examining whether this statement holds true in the case of intracellular reaction processes, we discuss the possible role of this force in the partitioning dynamics of bacterial chromosomal locus/plasmids during cell division. By introducing a dynamical system in which equations of motion for plasmids and a reaction-diffusion equation for concentration of a chemical mutually determine each other, we demonstrate that the chemophoresis force can contribute to a regular positioning of plasmids observed in experiments.

The scheme of this paper is as follows. In Sec. 2 for results, we derive an expression for the chemophoresis force in Sec. 2-1, and in Sec. 2-2, we consider a simple toy model of chemophoresis. In Sec. 2-3, we show that conditions for chemophoresis are satisfied in the intracellular reaction process. Sec. 2-4 discusses applications of chemophoresis force in the dynamics of bacterial chromosomal locus/plasmid partitioning during cell division. First, we perform an order estimation to examine the validity of the application of chemophoresis to bacterial chromosomal locus/plasmid partitioning. Next, we demonstrate that the chemophoresis force can contribute to the regular positioning of plasmids, which has been observed in experiments. In Sec. 3, a brief discussion on the relevance of chemophoresis to intracellular organization is presented. Discussions of the chemophoresis on the basis of thermodynamics and statistical mechanics are given in Appendix A and B, respectively.

2. Results

2-1. Chemophoresis

Consider organelles or macromolecules that have a number of binding sites on their surface for reactions to occur; for example, nucleoprotein complexes (NCs) have several promoter sites to bind transcription factors. Let us model these biological elements simply as beads with several reaction sites to which molecules attach themselves, as shown in

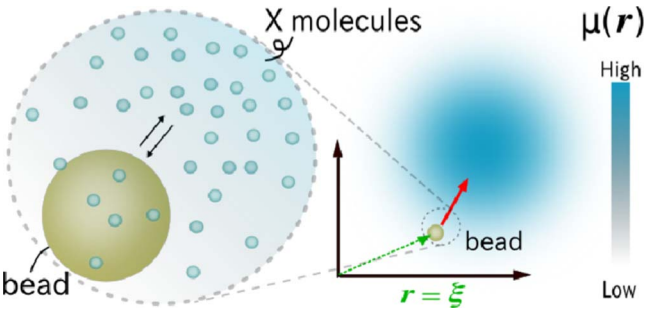

Figure 1 Schematic representation of our system. A bead is placed at $\boldsymbol{r} = \boldsymbol{\xi}$, and it moves in a d-dimensional space ($d = 1, 2, 3$). The adsorption reaction $\mathrm{X}(\boldsymbol{\xi}) + \mathrm{B} \underset{k_-}{\overset{k_+}{\rightleftharpoons}} \mathrm{Y}$ occurs on the surface of the bead.

Figure 1. The bead is placed at $\boldsymbol{r} = \boldsymbol{\xi}$ and moves in a d-dimensional space $\boldsymbol{r} \in \boldsymbol{R}^d$ ($d = 1, 2, 3$). We consider an isothermal process that is homogeneous over space at a given temperature T. We also consider a chemical bath containing a chemical X with a spatially dependent concentration $x(\boldsymbol{r})$ or, equivalently, the corresponding chemical potential $\mu(\boldsymbol{r})$. This gradient is assumed to be sustained externally. A molecule of X is attached to a binding site B on the bead and forms a complex Y (Fig. 1), as given by the reaction

$$\mathrm{X}(\boldsymbol{\xi}) + \mathrm{B} \underset{k_-}{\overset{k_+}{\rightleftharpoons}} \mathrm{Y}. \tag{1}$$

The molecular number of the complexes on the bead is denoted by N_y. Note that we define the bead as a macroscopic entity relative to an X molecule. To consider local-equilibrium conditions, we make the following assumptions. The "adsorption" reaction on the bead is considered to be a macroscopic event and N_y is the average molecular number that is averaged over a much longer time scale than the microscopic time scale of the reaction. Further, the bead is assumed to move sufficiently slowly so that the above reaction is in local chemical equilibrium at the position $\boldsymbol{r} = \boldsymbol{\xi}$. In other words, the time scales of diffusion of the X molecules (τ_{diff}) and the adsorption reaction (τ_{adsorb}) are much smaller than the time scale of the motion of the bead (τ_{bead}): $\tau_{diff}, \tau_{adsorb} \ll \tau_{bead}$. As long as the bead is in motion, it is in equilibrium with the reservoir at $\boldsymbol{r} = \boldsymbol{\xi}$.

With the assumption of the existence of local equilibrium, we can apply thermodynamics with spatially dependent thermodynamic variables. Indeed, at each position $\boldsymbol{\xi}$, the reaction process is described by the familiar classical Langmuir adsorption theory[37,38]; note that the theory has been successfully applied to DNA-protein binding equilibrium[37]. The grand potential at each position is given by $\Omega(\boldsymbol{\xi}) = F(\boldsymbol{\xi}) - y\mu(\boldsymbol{\xi})$, $d\Omega(\boldsymbol{\xi}) = dF(\boldsymbol{\xi}) - d(y\mu(\boldsymbol{\xi})) = -yd\mu(\boldsymbol{\xi})$, where $y = \dfrac{N_y}{V}$ (V: volume of the bead), $F(\boldsymbol{\xi})$ is the Helmholtz free energy, and $dF(\boldsymbol{\xi}) = \mu(\boldsymbol{\xi})dy$[39].

Now, consider a virtual displacement of the bead. Under an infinitesimal displacement $\xi \to \xi + d\xi$, the change in the grand potential is $d\Omega(\xi) = -y d\mu(\xi) = -y \nabla\mu(\xi) \cdot d\xi$. In other words, the position of the bead, ξ, is adopted as an effective independent variable instead of the chemical potential $\mu(\xi)$. Then, ξ is the work coordinate, while $-y\nabla\mu(\xi)$ is the force exerted on the bead by the external world balanced by the force generated by the reservoir chemical potential distribution $\mu(\xi)$; this force also acts on the bead. The reservoir-generated chemical gradient force per unit volume of the bead is

$$\boldsymbol{f}_{chem} = -\nabla\Omega(\xi) = y\nabla\mu(\xi). \tag{2}$$

This expression is obtained as follows. Consider a quasi-static infinitesimal displacement $d\xi$. Then, from the change in the grand potential, the maximum work done by the system on the external world through the reservoir is $d'W = y\nabla\mu(\xi)\cdot d\xi$. By considering that this work is done by the force that the reservoir exerts on the bead, i.e., $d'W = \boldsymbol{f}_{chem}\cdot d\xi$, the force formula in Eq. (2) is obtained. In other words, without an externally applied force, ξ evolves spontaneously so that $\Omega(\xi)$ monotonically decreases, that is, $d\Omega(\xi) < 0$. (see Appendix A for a detailed discussion in terms of the principle of maximum work). When we consider an overdamped system, where the kinetic energy of the bead is negligible, the phenomenological equation of motion is given by $\gamma\dot{\xi} = -\nabla\Omega(\xi) = y\nabla\mu(\xi)$; here, it is assumed that the friction constant resulting in dissipation is proportional to the velocity with the proportionality constant γ — the friction coefficient per unit volume of the bead.

Now, consider the condition for chemical equilibrium. Because $c = y + b = const.$, the dissociative constant is defined as $K = \frac{k_-}{k_+} = \frac{x(\xi)b}{y}$, where y is given by the Langmuir isotherm $y = y(x(\xi)) = c\frac{x(\xi)}{K + x(\xi)}$ (In statistical mechanics, the Langmuir isotherm is obtained as a function of the chemical potential $\mu(\boldsymbol{r})$ at $\boldsymbol{r} = \boldsymbol{\xi}$. We can derive the expression as a function of $\mu(\boldsymbol{r})$. Also see Appendix B.). If we consider the cooperative adsorption of n chemicals on the bead (given by $nX(\xi) + B \underset{k_-}{\overset{k_+}{\rightleftharpoons}} Y$), the isotherm for the adsorption is given as $y(x(\xi)) = c\frac{x(\xi)^n}{K^n + x(\xi)^n}$, where n denotes the Hill coefficient. Therefore, the equation of motion is written as

$$\gamma\dot{\xi} = c\frac{x(\xi)^n}{K^n + x(\xi)^n}\nabla\mu(\xi). \tag{3}$$

Eq. (3) is a general expression for the motion of an element that has a number of binding sites for chemical adsorption under the gradient of chemical potential. The theoretical description of the motion of the bead can be considered to be an extension of the Langmuir adsorption theory. We call this motion *chemophoresis* — similar to the nomenclature of typical 'phoresis' phenomena such as electrophoresis and thermophoresis. Because of the chemophoresis force, the direction of motion of the bead is such that the chemical potential is increased. Note that the force has an entropic origin from the viewpoint of statistical mechanics (also see Appendix B for an analysis of the force from the viewpoint of statistical mechanics).

When an additional external potential field $E(\boldsymbol{r})$ such as an elastic energy is applied to the bead, the relation $dF(\xi) = dE(\xi) + \mu(\xi)dy(\xi)$ holds (from the first law of thermodynamics). Accordingly, the grand potential of the system given by $\Omega(\xi) = F(\xi) - y(\xi)\mu(\xi)$ satisfies $d\Omega(\xi) = dF(\xi) - d(y(\xi)\mu(\xi)) = dE(\xi) - y(\xi)d\mu(\xi)$. Further, by taking into account thermal fluctuations, the equation of motion of the system is given by

$$\gamma\dot{\xi} = -\nabla E(\xi) + y(\xi)\nabla\mu(\xi) + \boldsymbol{\eta}(t), \tag{4}$$

with $<\boldsymbol{\eta}(t)> = 0$ and $<\boldsymbol{\eta}(t)\cdot\boldsymbol{\eta}(t')> = 2d\gamma k_B T\delta(t - t')$. Note that the equation is obtained as an extended form of the conventional one by considering the Helmholtz free energy as the thermodynamic potential for a closed system. It is straightforward to extend the present formula for multiple beads and multiple components, with interactions among the beads.

2-2. An example

We consider a simple toy model as an example of Eq. (4). We assume that a bead placed at $r = \xi$ is tethered and balanced at $r = 0$ in a one-dimensional space r by a restoration force produced by a linear spring; the force is represented by the harmonic potential $E(\xi) = \frac{a}{2}\xi^2$. The concentration of the chemical that reacts with the bead is assumed to be constant and is given by $x(r) = x_s \exp(\lambda(r - r_s))$, where $x_s = x(r_s)$ is the concentration of X at $r = r_s$, while the corresponding chemical potential is given by $\mu(r) = \bar{\mu} + k_B T \ln x(r)$. Here, $\bar{\mu}$ is the standard chemical potential. Then, by using Eq. (4) without considering thermal fluctuations, the equation of motion of the bead is obtained as $\gamma\dot{\xi} = y(\xi)\frac{d\mu}{dr}(\xi) - \frac{dE}{dr}(\xi) = \lambda k_B Tc\frac{x(\xi)^n}{K^n + x(\xi)^n} - a\xi$. Here, γ, c, K and a are the frictional coefficient, maximum adsorption concentration, dissociative constant, and spring constant, respectively. This equation can be rewritten as

$$\gamma\dot{\xi} = \frac{A}{1 + B\exp(-n\lambda(\xi - r_s))} - a\xi, \tag{5}$$

where $A = \lambda k_B Tc$, $B = \left(\frac{K}{x_s}\right)^n$. The steady state solution of the equation shows bistability as it includes a sigmoid function. If x_s is considered as a control parameter, upon increasing

x_s, Eq. (5) undergoes twofold bifurcation from monostable fixed points to bistable ones and then back to monostable states. A change in the chemical concentration leads to a change in the stable fixed position of the bead, which also shows bistability. This toy model can be used to explain how a stable position of an organelle undergoes bifurcation to a new location as the chemical concentration increases.

2-3. Conditions for chemophoresis

2-3-1. Condition (i): Relationships among time scales

The grand canonical description and local chemical equilibrium can be considered only under certain conditions. The following relationships must exist among time scales: (1) the time scale of adsorption τ_{adsorb} must be shorter than that of bead motion τ_{bead} in order for the adsorption reaction to reach equilibrium (approximately) before the bead moves, and (2) the time scale of bead motion must be much larger than that of the diffusion of the chemical adsorbed on the bead, i.e. $\tau_{bead} \gg \tau_{diff}$. This condition is necessary to assume that the motion of the bead is macroscopic under the chemical gradient, which itself diffuses in space. In living cells of interest, the molecular number is not large enough for the instantaneous chemical concentration to show large fluctuations. Hence, the macroscopic concentration relevant to the force is determined by the temporal average of the concentration of molecules over the diffusion time scale[40], and therefore, the above condition is important.

2-3-2. Condition (ii): Dominance of chemophoresis over thermal fluctuations

As long as the above conditions are satisfied, the direction of the gradient force, on an average, is such that the chemical potential increases, regardless of the magnitude of thermal fluctuations. However, the gradient force must be larger than the thermal noise in order for it to act effectively and to eliminate the need for long-time averaging to remove fluctuations. This leads to the following condition: the work done by the force must be greater than the thermal energy, i.e., $-V\int_{\xi_0}^{\xi} d\xi' y(\xi')\nabla\mu(\xi') > k_BT$ for a directional motion from ξ_0 to ξ (This inequality can also be derived from the steady-state solution of the Smoluchowski equation. For one-dimensional motion, the steady-state distribution of ξ is given by $P(\xi) = A\exp\left(-\frac{W(\xi)}{k_BT}\right)$. Here, A is a normalized factor and $W(\xi) = -V\int_{\xi_0}^{\xi} d\xi' y(\xi')\nabla\mu(\xi')$. If the position ξ_c that satisfies $W(\xi_c) \sim k_BT$ is smaller than the system size L, the distribution is concentrated at higher chemical potentials and the gradient force dominates over the thermal fluctuations. In such a case, the above inequality is obtained.). The concentration and chemical potential of chemical X are obtained as $x(r) = x_0\exp\left(-\frac{r}{r_c}\right)$ and $\mu(r) = \bar{\mu} + k_BT\ln x(r)$, respectively. Here, x_0 is the highest concentration and it corresponds to $r = 0$. In the case of one-dimensional motion from $r = 0$ to L, the above condition for the work is rewritten as follows: $\frac{N_c}{r_c}\int_0^L d\xi \frac{x_0^n e^{-n\frac{\xi}{r_c}}}{K^n + x_0^n e^{-n\frac{\xi}{r_c}}} > 1$ with $N_c = V c$. A straightforward calculation gives the inequality $\frac{N_c}{n}\ln\left(\frac{1+\left(\frac{x_0}{K}\right)^n}{1+\left(\frac{x_0}{K}\right)^n e^{-n\frac{L}{r_c}}}\right) > 1$, which can be rewritten in the form

$$\frac{x_0}{K} > \left(\frac{e^{\frac{n}{N_c}} - 1}{1 - e^{-n\left(\frac{L}{r_c}+\frac{1}{N_c}\right)}}\right)^{\frac{1}{n}}. \qquad (6)$$

This inequality is accompanied by the additional condition $N_c > \frac{r_c}{L}$. Note that the lower bound on $\frac{x_0}{K}$ decreases with $\frac{L}{r_c}$ and N_c, and the formula is valid over a wide range of $\frac{x_0}{K}$ values. Although this condition is valid for an exponentially decaying distribution, it is expected to be useful as an estimate of the order of magnitude.

2-4. An application of chemophoresis to plasmid/chromosomal locus partitioning

2-4-1. Estimate of the chemophoresis and the validity of the conditions

We consider applications of the chemophoresis force within a cell. As an example, consider the partitioning of chromosomal locus/plasmids in bacteria during cell division[8–24]. Here, the bead corresponds to a chromosomal locus/plasmid on which the relevant protein (X in the model) binds to form a NC (Y in the model) that is important for partitioning. For the application, the above-mentioned condition relating to the time scales (τ_{diff}, $\tau_{adsorb} \ll \tau_{bead}$) has to be satisfied. We first examine this condition.

In general, the time scale of protein binding equilibrium on bacterial DNA, τ_{adsorb}, is about the order of 1 (s). In Espeli *et al.*, Fiebig *et al.* and Elmore *et al.*, it has been suggested that the segregation of chromosomes is spatially restricted and the diffusion coefficient D of a chromosomal locus is estimated as 10^{-5}~10^{-4} ($\mu m^2/s$)[41–43]. The size of a NC, a, is assumed to be on the order of $a \sim 50$ (nm), so that τ_{bead} is estimated as $\tau_{bead} \sim \frac{a^2}{D} \sim \frac{0.05^2}{10^{-4}} \sim 25$ (s). Similarly, τ_{diff} is estimated as $\tau_{diff} \sim \frac{a^2}{D_x} \sim 10^{-3}$ (s), where D_x is the diffusion coefficient of proteins within the cytoplasm and is roughly

estimated as $D_x \sim 3.0$ ($\mu m^2/s$) (according to Elf *et al.*[44] and Xie *et al.*[45]). Therefore, $\tau_{diff} \ll \tau_{adsorb} \ll \tau_{bead}$, the condition for the chemophoresis is satisfied.

To examine the validity of condition (ii), we consider a specific example — the partitioning of bacterial chromosomal locus/plasmids to daughter cells by a Par system[8–24]. Here, the most ubiquitous partitioning system is the *parABS* partitioning loci (The Par system consists of three components: DNA binding protein ParB, ATPase ParA, and centromere-like site *parS*. ParB binds *parS*, spreads along the DNA, and forms a large NC around *parS*. ATP-bound ParA (ParA-ATP) can nonspecifically bind to DNA and interact with the ParB-*parS* NC[8–10,16–19,22–24].). Before cell division, daughter chromosomal locus/plasmids are precisely segregated by ATP-bound ParA (ParA-ATP) dynamic localization along with the associated (ParA-ATP)-NC interaction at the *parS* site on chromosome/plasmid. It has been suggested that ParA-ATP localization pulls *parS* chromosomal locus[10] or at least guides plasmids[24], but the mechanism by which ParA-ATP generates the driving force for chromosomal locus/ plasmid segregation has not been elucidated yet. Now, by regarding ParA-ATP as X and the NC (to be precise, ParB-*parS* NC mediated by ParA-ATP) as Y in our model, we will show that this driving force is naturally explained by the chemophoresis force.

To confirm the validity of our formula, we simply consider the steady concentration distribution of ParA-ATP to be $x(r) = x_0 \exp\left(-\frac{r}{r_c}\right)$ within $[0, L]$[9,10]. We then take $n = 2$ (because ParA-ATP cooperatively binds DNA)[46,47] and choose $K = 0.3$ (μM) on the basis of recent data obtained in Leonard *et al.*[46] and Castaing *et al.*[47]. Although the precise amount of ParA-ATP that binds DNA around the NC is unknown, $N_c \sim 10$ is a natural estimate since it has been suggested that a large amount of ParA is required to bind DNA around an NC. The localization scale r_c of ParA-ATP localization is not precisely known either and could vary across bacterial species. By assuming $\frac{L}{r_c} \sim 5$ from Toro *et al.*[9] and Fogel *et al.*[10], the condition in Eq. (6) can be rewritten as $\frac{x_0}{K} > 0.5$. Active protein binding generally occurs when a reasonable concentration $x_0 \sim K$ is reached and x_0 is larger than K so that the above inequality is satisfied. Therefore, the chemophoresis force dominates over the thermal fluctuations. Although the mechanism of ParA-ATP localization could depend on the species, the estimate suggests that the force plays a significant role in the partitioning of plasmids/chromosomal locus, independent of the specific molecular mechanisms. Further, we note that the above-mentioned "spring toy model" involving a gradient is applicable to the partitioning problem and may help explain the bifurcation of plasmids/chromosomal locus during cell division with a change in ParA-ATP localization.

2-4-2. Regular positioning determined by combining chemophoresis and the reaction-diffusion (RD) equation

Although the application mentioned here assumes a ParA-ATP steady distribution, the distribution sometimes shows pole-to-pole oscillation[17–24] or the formation of a different spatial pattern by a few plasmids[18,19,23]. Nevertheless, our theory is applicable to time-varying distributions because the force derived here leads to directional motion toward the ParA foci (peaks). Indeed, the directional motion has been suggested in Hatano *et al.*[24]. Furthermore, the present chemophoresis force is applicable to a RD system so that the plasmid is positioned according to the chemical concentration pattern. We shall discuss this in detail.

As mentioned in the previous subsection, we hypothesized that the chemophoresis force generated by a ParA-ATP concentration gradient drives plasmids in the direction of increased concentration. On the other hand, it has been observed that ParB-bound plasmids can stimulate the ATPase activity of ParA[16,19], which is similar to the Min system where MinE stimulates the ATPase activity of MinD homologous to ParA during cell division[34–36]. Hence, there exists feedback from plasmids to the ParA-ATP pattern dynamics. This means that the chemophoresis force generated by a ParA-ATP gradient acts on plasmids, whereas ParB on the plasmids can modulate the ParA-ATP distribution through chemical reactions; thus, there is a relation between the plasmids and the ParA-ATP dynamics. This interaction may lead to the regular spacing of plasmids, which is observed in experiments[18,19,23].

Here, we briefly study a dynamical system in which equations of motion for plasmids are coupled with a RD equation for ParA-ATP. Modeling studies in which biological details are taken into account will be reported elsewhere (Sugawara T. and Kaneko K., in preparation).

As was mentioned, ParA-ATP binds NC on a plasmid. ParA-ATP interacts with ParB which stimulates ParA ATPase activity at a catalytic rate k. Because ParA cannot bind the NC when it is not combined with ATP, free ParA products are released from the NC immediately after ATP hydrolysis. Thus the reaction formula can be written as

$$\mathrm{nParA\text{-}ATP + NC} \underset{k_-}{\overset{k_+}{\rightleftharpoons}} \mathrm{(ParA\text{-}ATP)_n - NC} \xrightarrow{\mathrm{k}} \mathrm{nParA + nADP + nP_i + NC}. \quad (7)$$

Through this reaction on the NC, a plasmid plays a role of a sink for ParA-ATP and induces a concentration gradient of this protein. Now, consider a one-dimensional space along the long cell axis and a plasmid i ($1 \le i \le N$) to be positioned at $r = \xi_i \in [0, L]$; Here, L is cell length. ParB is assumed to be collected and localized at the positions of NCs on plasmids. Denoting the concentration of ParA-ATP as u and that of ParB as b, the RD equation for the ParA-ATP concentra-

tion is given as follows:

$$\partial u_t(r,t) = D\nabla^2 u(r,t) + a - c\,u(r,t) - k\,b\sum_{i=1}^{N}\frac{u(\xi_i,t)^n}{K^n + u(\xi_i,t)^n}\,\delta(r-\xi_i), \quad (8)$$

where the first, second, and third terms represent the diffusion of ParA-ATP, its synthesis at a constant rate a, and linear degradation with a rate c, respectively; the last term denotes the inhibition by ParB on the NC.

On the other hand, from Eq. (3) and the representation for the chemical potential, $\mu = \bar{\mu} + k_B T \ln u$, the equations of motion for plasmids are given as

$$\gamma\dot{\xi}_i = b\,k_B T\frac{u(\xi_i,t)^n}{K^n + u(\xi_i,t)^n}\frac{\nabla u(\xi_i,t)}{u(\xi_i,t)} + \eta_i(t), \quad (9)$$

with $<\eta_i(t)> = 0$ and $<\eta_i(t)\,\eta_{i'}(t')> = 2\gamma k_B T\delta_{ii'}\delta(t-t')$.

We adopt the Neumann boundary condition (NBC) for the RD equation: $\nabla u(0) = \nabla u(L) = 0$. To confine the plasmids to a cell $r \in [0, L]$, we place reflection walls at $r = 0$ and $r = L$. This can be explicitly represented as

$$U_{bound}(r) := \begin{cases} 0 & 0 < r < L \\ \infty & \text{otherwise.} \end{cases} \quad (10)$$

Here, we set $a = 1$, $b = 10$, $c = 0.1$, $k = 1$, $D = 0.5$, $K = 0.5$, $n = 1$, $\gamma = 1000$, and $L = 10$ and choose unit energy so that $k_B T = 1$ (note that $\frac{a}{c}$ is larger than K, so that the chemophoresis force on the plasmids dominates over thermal fluctuations).

Partitioning of two replicated plasmids

First, we examine the case of $N = 1$ and 2 to examine how two replicated plasmids are separated into daughter cells. Figure 2 shows the dynamics and distribution of $u(r)$ and plasmid(s) along the long cell axis for the two N values. A plasmid is localized at the center of the cell for $N = 1$ whereas two plasmids are positioned approximately at distances of one-quarter and three-quarters of the cell axis for $N = 2$ (Fig. 2). These results are consistent with earlier reports on plasmid positioning during cell division[20,21].

Regular distribution of plasmids

Observation of such regular positioning of plasmids are not restricted to the cases of $N = 1$ and 2. For $N > 2$, stable regular distributions are formed as a result of the generation of the gradient of $u(r)$ by each plasmid. Figure 3 shows the distributions of $u(r)$ and plasmids for $N = 3 \sim 6$ along the long cell axis. Similarly, regular distribution of plasmids is achieved. A plasmid i is localized around a fixed position $r = \xi_i^s := \left(i - \frac{1}{2}\right)\frac{L}{N}$ ($i = 1, 2, ..., N$) and they appear to get arranged at an interval determined by $\frac{L}{N}$ (Fig. 3).

The regular positioning of plasmids is due to an effective interplasmid repulsive force. A plasmid, which acts as a sink for ParA-ATP, contributes to the formation of a concentration gradient in which the concentration increases with an increase in distance from the plasmid. The other plasmids are subjected to the chemophoresis force by the gradient in the direction of increasing ParA-ATP concentration so that the latter plasmids are pushed away from the former. Because the former is also subjected to the chemophoresis force by the gradient derived from the latter, there is mutual repulsion among the plasmids. As a result, the regular positioning of plasmids is achieved. In fact, on the basis of a recent experiment[14], the repulsive force between plasmids has been suggested to be cause of their regular positioning. The repulsive interaction between plasmids due to ParA-ATP and mediated by chemophoresis is consistent with such experimental results.

A concentration gradient of $u(r)$ is maintained around a plasmid (sink), while it is vanished due to NBC at the boundaries $r = 0$ and L. On other words, the plasmid is reflected at the boundaries by NBC and confined within $[0, L]$. Hence, an effective repulsive force from the boundaries acts on the plasmid even though gradients at the boundaries are vanished under NBC.

Here, we adopted the Neumann boundary condition $\nabla u(0) = \nabla u(L) = 0$. Although this boundary condition may be appropriate for intracellular dynamics, we have confirmed that the formation of the regular distribution is independent of the choice of boundary conditions. In fact, simulations of Eqs. (8) and (9) under the Dirichlet boundary condition $u(0) = u(L) = 0$ have demonstrated the regular distribution of plasmids as a result of chemophoresis.

3. Discussion

In this paper, we have demonstrated that when a chemical concentration gradient exists, a macroscopic element that acts as a scaffold for the absorption of a chemical is generally subjected to a thermodynamic force; the force makes it move in the direction of increasing chemical potential. We term this force chemophoresis force. The force has an entropic origin and thus is independent of the specific molecular mechanism, and it is expected to provide clues to the mechanism underlying mechanochemical coupling. We have derived a general formula for the magnitude of the force and have presented a few conditions that should be satisfied for the validity of this formula. The conditions are shown to be satisfied for the intracellular motion of macromolecules or organelles under a suitable chemical gradient. Further, the force is shown to be greater than the thermal fluctuation force.

In particular, we have applied chemophoresis to bacterial partitioning systems during cell division. By introducing a dynamical system consisting of equations of motion for plasmids and a reaction-diffusion equation that are mutually coupled, we have explained the regular positioning of plasmids, which has been observed in experiments. Because it

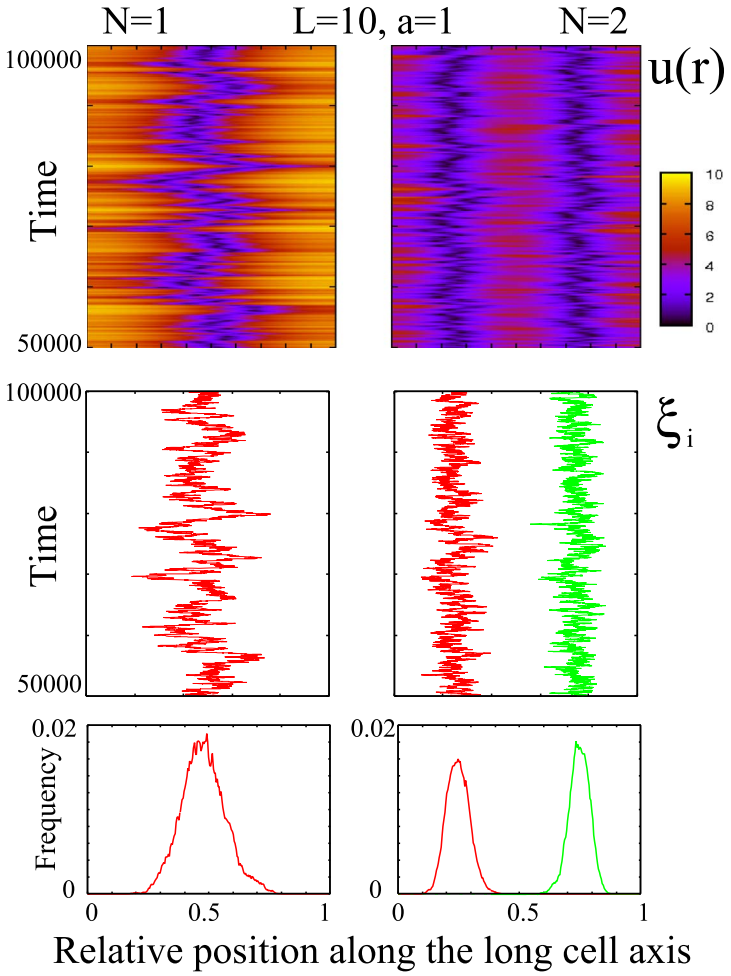

Figure 2 Dynamics and distribution along the long cell axis of $u(r)$ and plasmids.We show the cases of $N=1$ and 2. A plasmid is localized at the center of the cell for $N=1$ whereas two plasmids are positioned approximately at distances of one-quarter and three-quarters of the cell axis for $N=2$. Obtained from simulations of Eqs. (8) and (9) under the Neumann boundary condition, with the parameter values $a=1$, $b=10$, $c=0.1$, $k=1$, $D=0.5$, $K=0.5$, $n=1$, $\gamma=1000$, $L=10$, and $k_BT=1$.

has been reported that other organelles are also organized by ParA or its homologue[48,49], chemophoresis may contribute to these phenomena, too.

Here, we considered distributions of plasmids and ParA-ATP only along the long cell axis, and we studied equations of motion for plasmids coupled with the RD equation for ParA-ATP in one-dimensional space. It has been suggested that in reality, plasmids and ParA-ATP are restricted on a two-dimensional surface of the nucleoid of a host bacterial cell. A more realistic distribution can be obtained by taking into account two-dimensional plasmid motion under the gradient generated by ParB. In a future study, it is important to study a two-dimensional model by considering motions along both the longitudinal direction (parallel to the long cell axis) and transverse direction.

Furthermore, it is to be noted that our study does not exclude the possibility of the existence of other mechanisms for partitioning, such as the growth and shrinkage of ParA-ATP filaments[19]. To explain the regular positioning of the plasmids, the model used for the study of the growth and shrinkage of ParA-ATP filaments considers the polymerization of ParA-ATP along the long cell axis and the depolymerization of ParA-ATP by ParB on the plasmids[19]. In the model, it is sufficient to take into consideration only the polymerization-depolymerization in the longitudinal direction (parallel to the long cell axis), that is, in one-dimensional space. Indeed, chemophoresis is compatible with other possible mechanisms, and a combination of such mechanisms can enable the rapid and robust intracellular organization of macromolecules.

In applying chemophoresis to bacterial plasmid partitioning, we have focused particularly on the gradient generated and maintained by the regulation of ATP hydrolysis. Because the regulation of the gradient of a protein concentration by phospholylation-dephospholylation has been reported in Kholodenko[1], Carazo-Salas *et al.*[2], Caudron *et al.*[3] and Kalab and Heald[4] and suggested to be a general intracellular process, chemophoresis resulting from the reg-

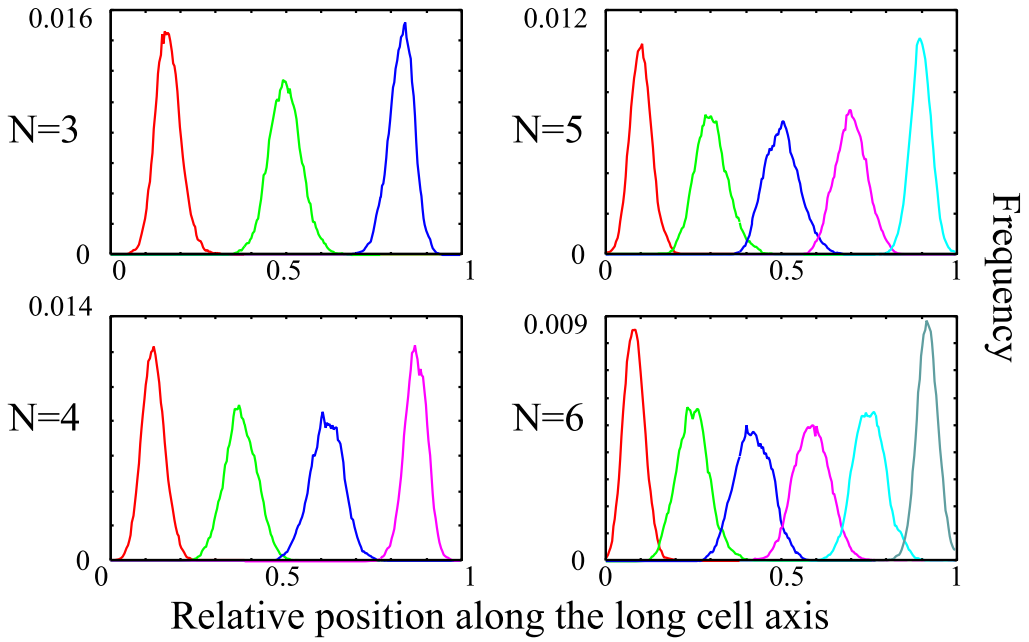

Figure 3 Distribution of plasmids along the long cell axis. We show the cases for $N=3\sim6$. The regular positioning of plasmids is achieved due to an effective inter-plasmid repulsive force and an effective repulsive force from the boundaries. A plasmid i is localized around a fixed position $r=\xi_i^s:=\left(i-\frac{1}{2}\right)\frac{L}{N}$ ($i=1, 2, ..., N$) and they appear to get arranged at an interval determined by $\frac{L}{N}$. Obtained from simulations of Eqs. (8) and (9) under the Neumann boundary condition, with the parameter values $a=1$, $b=10$, $c=0.1$, $k=1$, $D=0.5$, $K=0.5$, $n=1$, $\gamma=1000$, $L=10$, and $k_BT=1$.

ulation of phospholylation-dephospholylation, such as the regulation of the hydrolysis of ParA-ATP discussed in this paper, is expected to be ubiquitous in a variety of intracellular processes.

Apart from the chemophoresis reported here, there is another driving force generated by the concentration gradient; "diffusiophoresis", which is well-known in the transport of colloid[50–52]. In the diffusiophoresis, hydrodynamic effect is essential, while in the chemophoresis, chemical adsorption reaction is important. However, if the hydrodynamic effect is necessary, we can simply add the term into our formulation for chemophoresis. In the organization of plasmids, it appears that macroscopic hydrodynamic flow is not necessary. Indeed, an entropic effect caused by a gradient generated and maintained by the regulation of phospholylation-dephospholylation can explain the plasmid partitioning well.

It is important to note that in contrast to the hydrodynamic effect or other entropic forces such as the excluded volume effect, the chemophoresis force acts only on macroscopic elements (such as plasmids) to which proteins can bind. Because specific binding of a chemical is one of the most fundamental intracelluar processes for proper and robust functions, the generation of the chemophoresis force by such specific binding is expected to be a universal phenomenon that is responsible for the intracellular positioning of macromolecules and organelles.

Acknowledgments

The authors would like to thank Takagi, H., Awazu, A. & Ishihara, S. for useful discussions.

References

1. Kholodenko, B. N. Cell-signaling dynamics in time and space. *Nat. Rev. Mol. Cell Biol*. **7**, 165–176 (2006).
2. Carazo-Salas, R. E., Gruss, O. J., Mattaj, L. W. & Karsenti, E. Ran-GTP coordinates regulation of microtubule nucleation and dynamics during mitotic-spindle assembly. *Nat. Cell Biol*. **3**, 228–234 (2001).
3. Caudron, M., Bunt, G., Bastiaens, P. & Karsenti, E. Spatial coordination of spindle assembly by chromosome-mediated signaling gradients. *Science* **309**, 1373–1376 (2005).
4. Kalab, P. & Heald, R. The RanGTP gradient — a GPS for the mitotic spindle. *J. Cell Sci.* **121**, 1577–1586 (2008).
5. Niethammer, P., Bastiaens, P. & Karsenti, E. Stathmin-tubulin interaction gradients in motile and mitotic cells. *Science* **303**, 1862–1866 (2004).
6. Robbins, J. R., Monack, D., McCallum, S. J., Vegas, A., Pham, E., Goldberg, M. B. & Theriot, J. A. The making of a gradient: IcsA(VirG) polarity in *Shigella flexneri*. *Mol. Microbiol.* **41**, 861–872 (2001).
7. Gouin, E., Welch, M. D. & Cossart, P. Actin-based motility of intracellular pathogens. *Curr. Opin. Microbiol.* **8**, 35–45 (2005).
8. Mohl, D. A. & Gober, J. W. Cell cycle-dependent polar localization of chromosome partitioning proteins in *Caulobacter crescentus*. *Cell* **88**, 675–684 (1997).

9. Toro, E., Hong, S-H., McAdams, H. H. & Shapiro, L. *Caulobacter* requires a dedicated mechanism to initiate chromosome segregation. *Proc. Natl. Acad. Sci. USA* **105**, 15435–15440 (2008).
10. Fogel, M. A. & Waldor, M. K. A dynamic, mitotic-like mechanism for bacterial chromosome segregation. *Genes Dev.* **20**, 3269–3282 (2006).
11. Li, Y. & Austin, S. The P1 plasmid is segregated to daughter cells by a 'capture and ejection' mechanism coordinated with *Escherichia coli* cell division. *Mol. Microbiol.* **46**, 63–74 (2002).
12. Gordon, S., Rech, J., Lane, D. & Wright, A. Kinetics of plasmid segregation in *Escherichia coli*. *Mol. Microbiol.* **51**, 461–469 (2004).
13. Li, Y., Dabrazhynetskaya, A., Youngren, B. & Austin, S. The role of Par proteins in the active segregation of the P1 plasmid. *Mol. Microbiol.* **53**, 93–102 (2004).
14. Sengupta, M., Nielsen, H. J., Youngren, B. & Austin, S. P1 plasmid segregation: accurate redistribution by dynamic plasmid pairing and separation. *J. Bacteriol.* **192**, 1175–1183 (2010).
15. Ebersbach, G. & Gerdes, K. The double *par* locus of virulence factor pB171: DNA segregation is correlated with oscillation of ParA. *Proc. Natl. Acad. Sci. USA* **98**, 15078–15083 (2001).
16. Hunding, A., Ebersbach, G. & Gerdes, K. A mechanism for ParB-dependent waves of ParA, a protein related to DNA segregation during cell division in prokaryotes. *J. Mol. Biol.* **329**, 35–43 (2003).
17. Ebersbach, G. & Gerdes, K. Bacterial mitosis: partitioning protein ParA oscillates in spiral-shaped structures and positions plasmids at mid-cell. *Mol. Microbiol.* **52**, 385–398 (2004).
18. Ebersbach, G., Ringgaard, S., Møller-Jensen, J., Wang, Q., Sherratt, D. J. & Gerdes, K. Regular cellular distribution of plasmids by oscillating and filament-forming ParA ATPase of plasmid pB171. *Mol. Microbiol.* **61**, 1428–1442 (2006).
19. Ringgaard, S., van Zon, J., Harward, M. & Gerdes, K. Movement and equipositioning of plasmids by ParA filaments disassembly. *Proc. Natl. Acad. Sci. USA* **106**, 19369–19374 (2009).
20. Niki, H. & Hiraga, S. Subcellular distribution of actively partitioning F plasmid during the cell division cycle in *E. coli*. *Cell* **90**, 951–957 (1997).
21. Gordon, G. S., Sitnikov, D., Webb, C. D., Teleman, A., Straight, A., Losick, R., Murray, A. W. & Wright, A. Chromosome and low copy plasmid segregation in *E. coli*: visual evidence for distinct mechanisms. *Cell* **90**, 1113–1121 (1997).
22. Lim, G. E., Derman, A. I. & Pogliano, J. Bacterial DNA segregation by dynamic SopA polymers. *Proc. Natl. Acad. Sci. USA* **102**, 17658–17663 (2005).
23. Adachi, S., Hori, K. & Hiraga, S. Subcellular positioning of F plasmid mediated by dynamic localization of SopA and SopB. *J. Mol. Biol.* **356**, 850–863 (2006).
24. Hatano, T., Yamaichi, Y. & Niki, H. Oscillating focus of SopA associated with filamentous structure guides partitioning of F plasmid. *Mol. Microbiol.* **64**, 1198–1213 (2007).
25. A. Turing The chemical basis of morphogenesis. *Philos. Trans. R. Soc. London B* **237**, 37–72 (1952).
26. Hale, C. A., Meinhardt, H. & de Boer, P. J. Dynamic localization cycle of the cell division regulator MinE in *Escherichia coli*. *EMBO J.* **20**, 1563–1572 (2001).
27. Meinhardt, H. & de Boer, P. Pattern formation in *Escherichia coli*: A model for the pole-to-pole oscillations of Min proteins and the localization of the division site. *Proc. Natl. Acad. Sci. USA* **98**, 14202–14207 (2001).
28. Howard, M., Rutenberg, A. D. & de Vet, S. Dynamic compartmentalization of bacteria: accurate division in *E. coli*. *Phys. Rev. Lett.* **87**, 278102 (2001).
29. Kruse, K. A dynamic model for determining the middle of *Escherichia coli*. *Biophys. J.* **82**, 618–627 (2002).
30. Huang, K. C., Meir, Y. & Wingreen, N. S. Dynamic structures in *Escherichia coli*: Spontaneous formation of MinE rings and MinD polar zones. *Proc. Natl. Acad. Sci. USA* **100**, 12724–12728 (2003).
31. Howard, M. A mechanism for polar protein localization in bacteria. *J. Mol. Biol.* **335**, 655–663 (2004).
32. Drew, D. A., Osborn, M. J. & Rothfield, L. I. A polymerization–depolymerization model that accurately generates the self-sustained oscillatory system involved in bacterial division site placement. *Proc. Natl. Acad. Sci. USA* **102**, 6114–6118 (2005).
33. Kerr, R. A., Levine, H., Sejnowski, T. J. & Rappel, W.-J. Division accuracy in a stochastic model of Min oscillations in *Escherichia coli*. *Proc. Natl. Acad. Sci. USA* **103**, 347–352 (2006).
34. Lutkenhaus, J. Assembly dynamics of the bacterial MinCDE system and spatial regulation of the Z ring. *Annu. Rev. Biochem.* **76**, 539–562 (2007).
35. Howard, M. & Kruse, K. Cellular organization by self-organization: mechanisms and models for Min protein dynamics. *J. Cell Biol.* **168**, 533–536 (2005).
36. Kruse, K., Howard, M. & Margolin, W. An experimentalist's guide to computational modelling of the Min system. *Mol. Microbiol.* **63**, 1279–1284 (2007).
37. Phillips, R., Kondev, J. & Theriot, J. *Physical Biology of the Cell* (Garland Science, New York, 2008).
38. Ernst, B., Bodmann, J., Dick, D. P. & Dick, Y. P. An adsorption isotherm from a micro-state model. *Adsorption*, **10**, 277–286 (2004).
39. Callen, H. B. *Thermodynamics*, Sec. 14.2 (John Wiley & Sons, New York, 1960).
40. Tostevin, F., Wolde, P. R. & Howard, M. Fundamental limits to position determination by concentration gradients. *PLoS. Compute. Biol.* **3**, e78 (2007).
41. Espeli, O., Mercier, R. & Boccard, F. DNA dynamics vary according to macrodomain topography in the *E. coli* chromosome. *Mol. Microbiol.* **68**, 1418–1427 (2008).
42. Fiebig, A., Keren, K. & Theriot, J. Fine-scale time-lapse analysis of the biphasic, dynamic behavior of the two *Vibrio cholerae* chromosomes. *Mol. Microbiol.* **60**, 1164–1178 (2006).
43. Elmore, S., Müller, M., Vischer, N., Odijk, T. & Woldringh, C. L. Single-particle tracking of *oriC*-GFP fluorescent spots during chromosome segregation in *Escherichia coli*. *J. Struct. Biol.* **151**, 275–287 (2005).
44. Elf, J., Li, G.-W. & Xie, X. S. Probing transcription factor dynamics at the single-molecule level in a living cell. *Science*, **316**, 1191–1194 (2007).
45. Xie, X. S., Choi, P. J., Li, G.-W., Lee, N. K. & Lia, G. Single-molecule approach to molecular biology in living bacterial cells. *Annu. Rev. Biochem.* **37**, 417–444 (2008).
46. Leonard, T. A., Butler, P. J. & Löwe, J. Bacterial chromosome segregation: structure and DNA binding of the Soj dimer — a conserved biological switch. *EMBO J.* **24**, 270–282 (2005).
47. Castaing, J.-P., Bouet, J.-Y. & Lane, D. F plasmid partition depends on interaction of SopA with non-specific DNA. *Mol. Microbiol.* **70**, 1000–1011 (2008).
48. Thompson, S. R., Wadhams, G. H. & Armitage, J. P. The positioning of cytoplasmic protein clusters in bacteria. *Proc. Natl. Acad. Sci. USA* **103**, 8209–8214 (2006).
49. Savage, D. F., Afonso, B., Chen, A. H. & Silver, P. A. Spatially

ordered dynamics of the bacterial carbon fixation machinery. *Science* **327**, 1258–1261 (2010).
50. Anderson, J. Colloid transport by interfacial forces. *Annu. Rev. Fluid Mech.* **21**, 61–99 (1989).
51. Jülicher, F. & Prost, J. Generic theory of colloidal transport. *Eur. Phys. J. E* **29**, 27–36 (2009).
52. Palacci, J., Abécassis, B., Cottin-Bizonne, C., Ybert, C. & Bocquet, L. Colloidal motility and pattern formation under rectified diffusiophoresis. *Phys. Rev. Lett.* **104**, 138302 (2010).

Appendix A

Discussion of the variational principle for grand potential with the principle of maximum work

It is well known that the grand potential is a thermodynamic potential in terms of natural variables T, μ and surface area. Following the standard thermodynamic principle of maximum work, we will discuss the variational principle for the grand potential.

Consider a thermodynamic system composed of a bead with a surface as shown in Fig. 1 and that it is maintained in equilibrium during its motion. Therefore, the temperature and chemical potential of the system are always balanced by those of the reservoir, that is, $T_{system} = T, \mu_{system} = \mu(\boldsymbol{\xi})$. By the assumption of local equilibrium, several thermodynamic variables can be defined in the d-dimensional space.

The precise definition of the grand potential is as follows:

$$\Omega(T,\mu) := \min_{y} [F(T,y) - y\mu] \tag{11}$$

This is the precise representation for the Legendre transformation from $F(T,y)$, the Helmholtz free energy in terms of natural variables (T,y), to $\Omega(T,\mu)$ in terms of natural variables (T,μ). The determined y^* and $F(T,y^*) - y^*\mu$ by the minimum condition are identical to the Langmuir isotherm and the grand potential, respectively.

The principle of maximum work represents the second law of thermodynamics in terms of the work obtained by the change of y under an isothermal process:

$$W_{max}(T, y_1 \to y_2) = F(T,y_1) - F(T,y_2) \tag{12}$$

When y is quasistatically changed from y_1 as a function of μ_1 to *any* y_2 by moving the position of the bead from $\boldsymbol{\xi}_1$ to $\boldsymbol{\xi}_2$ via the force $\boldsymbol{f}$ exerted by the external world, the work performed by the system on the external world is given as:

$$W(T,\mu_1 \to \mu_2) = -\int_{\xi_1}^{\xi_2} \boldsymbol{f}\cdot d\boldsymbol{\xi} = W_{max}(T, y_1 \to y_2) - \left(-\int_{y_1\mu_1}^{y_2\mu_2} d(y\mu)\right) \tag{13}$$

The first term represents the total work that the system can perform, and the second term represents the work that the system performs on the reservoir. The latter work can be interpreted as the integration of the potential energy of the system $-y(\boldsymbol{\xi})\mu(\boldsymbol{\xi})$ from $\boldsymbol{\xi}_1$ to $\boldsymbol{\xi}_2$.

We consider maximizing $W(T,\mu_1 \to \mu_2)$ by changing y_2 determined arbitrarily so far and then determining it as a function of (T, μ_2). The maximum work is expressed in terms of natural variables T, μ as $W_{max}(T,\mu_1 \to \mu_2)$, as follows:

$$\begin{aligned} W_{max}(T,\mu_1 \to \mu_2) &= \max_{y_2} W(T,\mu_1 \to \mu_2) \\ &= \max_{y_2} [W_{max}(T, y_1 \to y_2) + y_2\mu_2 - y_1\mu_1] \\ &= F(T,\mu_1) - y_1\mu_1 - \min_{y_2} [F(T,\mu_2) - y_2\mu_2] \\ &= \Omega(T,\mu_1) - \Omega(T,\mu_2) \end{aligned} \tag{14}$$

Next, we consider the situation in which the force $\boldsymbol{f}$ exerted by the external world vanishes ($\boldsymbol{f} = \boldsymbol{0}$) and the change $\mu \to \mu'$ occurs spontaneously. In this case, $W(T,\mu \to \mu') = 0$ because $\boldsymbol{f} = \boldsymbol{0}$.

$$\begin{aligned} &\therefore\ W_{max}(T,\mu \to \mu') \geq W(T,\mu \to \mu') = 0 \\ &\Leftrightarrow\ \Omega(T,\mu') - \Omega(T,\mu) \leq 0 \end{aligned} \tag{15}$$

For an infinitesimal displacement $\boldsymbol{\xi} \to \boldsymbol{\xi} + d\boldsymbol{\xi}$, the following inequality is satisfied:

$$d\Omega(T,\mu) = \nabla\Omega(T,\boldsymbol{\xi})\cdot d\boldsymbol{\xi} \leq 0 \tag{16}$$

Therefore, for a displacement per unit time $\dot{\boldsymbol{\xi}}$,

$$\dot{\Omega}(T,\boldsymbol{\xi},\dot{\boldsymbol{\xi}}) = \nabla\Omega(T,\boldsymbol{\xi})\cdot\dot{\boldsymbol{\xi}} \leq 0 \tag{17}$$

Appendix B

Discussion of Chemophoresis from the Viewpoint of Statistical Mechanics

Although we considered only the thermodynamic approach to obtain the chemophoresis force, the obtained force can also be determined by using a statistical-mechanics approach.

Following the standard technique, we coarse-grain the original system by tracing out some coordinates, to determine an effective potential for slower coordinates. For example, we trace out some coordinates $\{\boldsymbol{r}_i\}_{1\le i\le N}$ for a system with a Hamiltonian $H(\{\boldsymbol{r}_i\}, \{\boldsymbol{R}_j\})$ when some coordinates $\{\boldsymbol{R}_j\}_{1\le j\le M}$, which are much slower than $\{\boldsymbol{r}_i\}$, are fixed. An effective potential for $\{\boldsymbol{R}_j\}$, $U_{eff}(\{\boldsymbol{R}_j\})$, is defined as follows:

$$U_{eff}(\{\boldsymbol{R}_j\}) := -k_B T \ln P(\{\boldsymbol{R}_j\}) \tag{18}$$

Here, $P(\{\boldsymbol{R}_j\})$ is the probability distribution of $\{\boldsymbol{R}_j\}$:

$$P(\{\boldsymbol{R}_j\}) := \frac{e^{-\frac{U_{eff}(\{\boldsymbol{R}_j\})}{k_B T}}}{\int \prod_{k=1}^{M} d\boldsymbol{R}_k e^{-\frac{U_{eff}(\{\boldsymbol{R}_k\})}{k_B T}}} = \frac{1}{Q}\int \prod_{i=1}^{N} d\boldsymbol{r}_i e^{-\frac{H(\{\boldsymbol{r}_i\},\{\boldsymbol{R}_j\})}{k_B T}} \tag{19}$$

where Q is the partition function of the original system $(\{\boldsymbol{r}_i\}, \{\boldsymbol{R}_j\})$; $Q := \int \prod_{i=1}^{N} d\boldsymbol{r}_i \prod_{j=1}^{M} d\boldsymbol{R}_j e^{-\frac{H(\{\boldsymbol{r}_i\},\{\boldsymbol{R}_j\})}{k_B T}}$. One can see that the effective potential $U_{eff}(\{\boldsymbol{R}_j\})$ corresponds to the free energy as a function of $\{\boldsymbol{R}_j\}$ that is obtained by canonical-averaging for $\{\boldsymbol{r}_i\}$ when $\{\boldsymbol{R}_j\}$ is fixed. A mean force acts on $\{\boldsymbol{R}_j\}$ so as to minimize $U_{eff}(\{\boldsymbol{R}_j\})$, to attain equilibrium. The force acting on $\{\boldsymbol{R}_j\}$ is obtained as

$$\boldsymbol{f}_j = \frac{\partial U_{eff}(\{\boldsymbol{R}_k\})}{\partial \boldsymbol{R}_j} \tag{20}$$

As will be seen below, the same formula as that derived from the thermodynamic approach is obtained for the chemophoresis force by defining an effective potential for the bead's coordinate much slower than chemical binding equilibrium.

As discussed earlier in this paper, consider a "bead", which is a macroscopic entity that has binding sites for chemical adsorption reactions to occur on its surface. The bead is placed at $\boldsymbol{r} = \boldsymbol{\xi}$ and moves in a d-dimensional space $\boldsymbol{r} \in \boldsymbol{R}^d$ ($d = 1, 2, 3$). We consider an isothermal process that is homogeneous over space at a given temperature T; we also consider a chemical bath with a chemical X having a spatially dependent concentration $x(\boldsymbol{r})$, or equivalently, the corresponding chemical potential $\mu(\boldsymbol{r})$. The concentration gradient is assumed to be sustained externally.

First, we show that for a general situation, an effective potential for the bead's motion is equivalent to the grand potential and that the mean force defined in the same way as the above procedure corresponds to the chemophoresis force derived from the thermodynamic approach. Next, as a simple example, we will obtain a concrete representation of the chemophoresis force by using a two-state system.

Consider a system with a binding site i ($1 \le i \le N_c$) on which N_i molecules of chemical X bind. The binding energy per molecule and Hamiltonian of the system are represented as ε_i and $H(\{\varepsilon_i\}_{1\le i\le Nc})$, respectively. In order to obtain an effective potential for $\boldsymbol{\xi}$, we perform grand canonical averaging for chemical adsorption when the bead's coordinate $\boldsymbol{r} = \boldsymbol{\xi}$ is fixed because the bead is assumed to move sufficiently slowly so that local chemical equilibrium can be assumed to exist at each position $\boldsymbol{r} = \boldsymbol{\xi}$ during the adsorption reaction: $\tau_{bead} \gg \tau_{adsorb}$. As discussed above, we can define an effective potential $U_{eff}(\boldsymbol{\xi})$ as

$$U_{eff}(\boldsymbol{\xi}) := -k_B T \ln P(\boldsymbol{\xi}) \tag{21}$$

Here, $P(\boldsymbol{\xi})$ is the probability distribution of $\boldsymbol{\xi}$:

$$P(\boldsymbol{\xi}) := \frac{e^{-\frac{U_{eff}(\boldsymbol{\xi})}{k_B T}}}{\int d\boldsymbol{\xi}' e^{-\frac{U_{eff}(\boldsymbol{\xi}')}{k_B T}}} = \frac{\Xi(\boldsymbol{\xi})}{\int d\boldsymbol{\xi}' \Xi(\boldsymbol{\xi}')} = \frac{e^{-\frac{\Omega(\boldsymbol{\xi})}{k_B T}}}{\int d\boldsymbol{\xi}' e^{-\frac{\Omega(\boldsymbol{\xi}')}{k_B T}}} \tag{22}$$

where $\Xi(\boldsymbol{\xi})$ is a partition function of the system obtained by summing over microscopic states $(\{\varepsilon_i\}, \{N_i\})$ and is given by

$$\Xi(\boldsymbol{\xi}) := \sum_{\varepsilon_i, N_i} e^{-\frac{H(\{\varepsilon_i\}) - \sum_{i=1}^{N} \mu(\boldsymbol{\xi}) N_i}{k_B T}} \tag{23}$$

and $\Omega(\boldsymbol{\xi})$ is the grand potential

$$\Omega(\boldsymbol{\xi}) = -k_B T \ln \Xi(\boldsymbol{\xi}) \tag{24}$$

We can see that $U_{eff}(\boldsymbol{\xi}) = \Omega(\boldsymbol{\xi}) + const.$ and that $\Omega(\boldsymbol{\xi})$ is equal to $U_{eff}(\boldsymbol{\xi})$ except for a constant factor. Therefore, there is an effective force per volume, $\boldsymbol{f}$, that is equal to the chemophoresis force $\boldsymbol{f}_{\text{chem}}$, and it is written as

$$\boldsymbol{f}_{\text{chem}} = -\frac{1}{V}\nabla U_{eff}(\boldsymbol{\xi}) = -\frac{1}{V}\nabla \Omega(\boldsymbol{\xi}) = y(\mu(\boldsymbol{\xi}))\nabla \mu(\boldsymbol{\xi}), \tag{25}$$

$$y(\mu(\boldsymbol{\xi})) := -\frac{1}{V}\left(\frac{\partial \Omega}{\partial \mu}\right)_T = \frac{k_B T}{V}\frac{1}{\Xi}\left(\frac{\partial \Xi}{\partial \mu}\right)_T > 0. \tag{26}$$

Here, the bead can move in a direction that decreases $U_{eff}(\boldsymbol{\xi})$ as a result of the increase in $\mu(\boldsymbol{\xi})$ when the gradient of $\mu(\boldsymbol{r})$ is sustained. This is consistent with the result of the thermodynamic approach. The chemophoresis force then acts to decrease the grand potential in the presence of the chemical potential gradient. The effective potential $U_{eff}(\boldsymbol{\xi})$ is obtained through coarse-graining by grand canonical averaging for chemical adsorption by maintaining $\boldsymbol{\xi}$ fixed. This is valid when the time scale of chemical equilibrium is much smaller than that of the bead's motion. This procedure is equivalent

to the above mentioned conventional coarse-graining one and can be used to obtain an effective potential for slow coordinates.

Next, as a simple example, we obtain a concrete representation of the chemophoresis force using a two-state system, with bound and unbound states, per binding site. If the system is in the bound (unbound) state, the change in its energy is $\varepsilon(0)$. In other words, this chemical is attached to the binding sites on the bead and thus forms a complex Y (see Fig. 1), as given by Reaction (1). For a system with only one binding site, the partition function is obtained by summing over the microscopic states $(\varepsilon_1, N_1) = (\varepsilon, 1), (0, 0)$:

$$\Xi(\boldsymbol{\xi}) = \sum_{\varepsilon_1, N_1} e^{-\frac{\varepsilon_1 - \mu(\boldsymbol{\xi})N_1}{k_B T}} = 1 + e^{-\frac{\varepsilon - \mu(\boldsymbol{\xi})}{k_B T}} . \qquad (27)$$

Assuming that the chemical adsorption reactions at the N_c binding sites are independent of each other, the partition function and the grand potential for the system with N_c binding sites are written as

$$\Xi(\boldsymbol{\xi}) = \left(1 + e^{-\frac{\varepsilon - \mu(\boldsymbol{\xi})}{k_B T}} \right)^{N_c}, \qquad (28)$$

$$\Omega(\boldsymbol{\xi}) = -k_B T \ln \Xi(\boldsymbol{\xi}) = -N_c k_B T \ln \left(1 + e^{-\frac{\varepsilon - \mu(\boldsymbol{\xi})}{k_B T}} \right). \qquad (29)$$

Eventually, the chemophoresis force is written as

$$\boldsymbol{f}_{\text{chem}} = y(\mu(\boldsymbol{\xi}))\nabla\mu(\boldsymbol{\xi}), \quad y(\mu(\boldsymbol{\xi})) = c\,\frac{e^{-\frac{\varepsilon - \mu(\boldsymbol{\xi})}{k_B T}}}{1 + e^{-\frac{\varepsilon - \mu(\boldsymbol{\xi})}{k_B T}}} . \qquad (30)$$

Here, $c := \frac{N_c}{V}$. Using $\mu = \bar{\mu} + k_B T \ln N \left(x = \frac{N}{V} \right)$, and $y(x(\boldsymbol{\xi})) = c\frac{x(\boldsymbol{\xi})}{K + x(\boldsymbol{\xi})}$ obtained by considering chemical kinetics, we get the relation

$$K = \frac{k_-}{k_+} = \frac{1}{V} e^{-\frac{\varepsilon - \bar{\mu}}{k_B T}} . \qquad (31)$$

Similarly, for the cooperative binding case $\mathrm{nX}(\boldsymbol{\xi}) + \mathrm{B} \underset{k_-}{\overset{k_+}{\rightleftharpoons}} \mathrm{Y}$, the Langmuir isotherm is as follows:

$$y(\mu(\boldsymbol{\xi})) = c\,\frac{e^{-n\frac{\varepsilon - \mu(\boldsymbol{\xi})}{k_B T}}}{1 + e^{-n\frac{\varepsilon - \mu(\boldsymbol{\xi})}{k_B T}}} . \qquad (32)$$

From the above discussion, we can see that $\boldsymbol{f}_{\text{chem}}$ is a force with an entropic origin.